

Adipose-derived mesenchymal stem cells may reduce intestinal epithelial damage in ulcerative colitis by communicating with macrophages and blocking inflammatory pathways: an analysis *in silico*

Nan Zhang^{1,*}, Yixuan Chen^{1,*}, Chengyu Huang^{1,*}, Mengxin Wei^{1,*}, Ting Li¹, Yufeng Lv², Qiong Song^{1,3}, Shaowen Mo^{1,3}

¹YuanDong International Academy of Life Sciences, Nanning 530000, Guangxi, China

²Department of Oncology, Foresea Life Insurance Guangxi Hospital, Nanning 530000, Guangxi, China

³Chinese Academy of Science Center for Excellence in Brain Science and Intelligence Technology, Chinese Academy of Science, Shanghai 200031, China

*Equal contribution

Correspondence to: Yufeng Lv, Qiong Song, Shaowen Mo; **email:** tougaozhuanrong_lv@126.com, <https://orcid.org/0000-0001-5542-1783>; qsong@ydlife.org; swmo@ydlife.org

Keywords: ulcerative colitis, inflammatory disease, colonic mucosa, submucosa, pathogenesis

Received: July 13, 2021

Accepted: February 8, 2022

Published: March 22, 2022

Copyright: © 2022 Zhang et al. This is an open access article distributed under the terms of the [Creative Commons Attribution License](https://creativecommons.org/licenses/by/3.0/) (CC BY 3.0), which permits unrestricted use, distribution, and reproduction in any medium, provided the original author and source are credited.

ABSTRACT

Ulcerative colitis is a chronic, non-specific inflammatory disease that affects mainly the colonic mucosa and submucosa. The pathogenesis of ulcerative colitis is unclear, which limits the development of effective treatments. In this study, single-cell sequencing data from 18 ulcerative colitis samples and 12 healthy controls were downloaded from the Single Cell Portal database, cell types were defined through cluster analysis, and genes in each cluster that were differentially expressed in ulcerative colitis were identified. These genes were enriched in functional pathways related to apoptosis, immunity and inflammation. Analysis using iTALK software suggested extensive communication among immune cells. Single-cell sequencing data from adipose-derived mesenchymal stem cells from three healthy female donors were obtained from the Sequence Read Archive database. The SingleR package was used to identify different cell types, for each of which a stemness score was calculated. Pseudotime analysis was performed to infer the trajectory of cells. SCENIC software was used to identify the gene regulatory network in adipose-derived mesenchymal stem cells, and iTALK software was performed to explore the relationship among macrophages, adipose-derived mesenchymal stem cells and enterocytes. Molecular docking confirmed the possibility of cell-cell interactions via binding between surface receptors and their ligands. The bulk data were downloaded and analyzed to validate the expression of genes. Our bioinformatics analyses suggest that ulcerative colitis involves communication between macrophages and enterocytes via ligand-receptor pairs. Our results further suggest that adipose-derived mesenchymal stem cells may alleviate ulcerative colitis by communicating with macrophages to block inflammation.

INTRODUCTION

Ulcerative colitis (UC) is a chronic, non-specific inflammatory disease that affects mainly the

colonic mucosa and submucosa [1]. UC tends to recur and often progresses to cancer [2]. Current treatments include aminosalicic acid, immunosuppressants and adrenal glucocorticoids,

but they are often ineffective and the disease can recur [3].

The pathogenesis of UC is unclear. Pathological examination of intestinal tissues during active UC shows extensive damage to intestinal epithelial cells as well as diffuse inflammation [2, 4]. The intestinal mucosal acts as an immune and mechanical barrier [5] that maintains the stability of the intestinal flora and host immune tolerance toward intestinal microbes [6]. The chronic inflammation in UC can weaken the tight junctions between epithelial cells [7], leading to the destruction of the mucus layer on the surface of the intestinal epithelium [8]. Apoptosis and autophagy may also contribute to damage of the intestinal mucosa in UC [9].

Immune cells appear capable of influencing the course of UC. The subtype of monocytes called macrophages regulate immune responses in the intestinal micro-environment in UC [10]. Macrophages remove apoptotic cells [11] and regulate inflammatory processes [9]. Adipose-derived mesenchymal stem cells (ADMSCs) regulate macrophage function, and they down-regulate pro-inflammatory factors (INF γ , IL-6 and IL-8) while up-regulating anti-inflammatory factors (IL-10, IL-4), thereby weakening the local inflammatory response [12]. Clarifying the roles and interactions of macrophages and ADMSCs in UC may help clarify how the disease occurs and progresses, which may lead to therapeutic targets.

In this bioinformatics study, we found evidence that macrophages may damage the intestinal mucosal barrier by promoting inflammation and intestinal epithelial cell apoptosis/autophagy, likely contributing to UC. We found evidence that, conversely, ADMSCs may communicate with macrophages to block inflammation and thereby alleviate UC.

MATERIALS AND METHODS

Single cell data collection and quality control

Single-cell RNA sequencing data from colon biopsies of 18 patients with UC and 12 healthy individuals were collected from the Single Cell Portal database (accession number SCP259) [1]. Single-cell RNA sequencing data from ADMSCs from thigh source of three healthy female donors were obtained from the Sequence Read Archive database (accession number SRP148833) [13].

Sequencing data were subjected to quality control based on the following criteria [14]: gene number between 200 and 6000, unique molecular identifiers (UMI)

count > 1000, and mitochondrial gene percentage < 0.1. All 23 samples with sequencing data were used for cell-clustering analysis.

Dimensional reduction, clustering and cell type identification

The most variable genes in single cells were identified as described [15]. In brief, the average expression and dispersion of each gene were calculated, then the genes were assigned to eight bins based on their expression. The “NormalizeData” function in Seurat [14] was used to normalize the expression matrix of single cells. The expression matrix was multiplied by 10000 using the “LogNormalize” function, then divided by the size of the total library, so that different cells could be compared. The expression levels of highly variable genes were scaled and centered using the “ScaleData” function in order to exclude the influence of mitochondrial genes and the total number of molecules detected within a cell.

Data were visualized in two dimensions using the “uniform manifold approximation and projection for dimension reduction” (UMAP) method. The SingleR package in R (version 0.2.2) was used to independently infer the cell source and identify the type of each single cell, based on the “Immgen” data set [15]. The “Findallmarkers” function in Seurat version 3.1.2 was used to identify differentially expressed genes (DEGs) in UC. DEGs were defined as those showing $|\log_2(\text{fold change})| > 1$ and $P < 0.05$ with respect to controls.

To uncover the potential biological significance of DEGs, their enrichment in functional pathways was examined using the Kyoto Encyclopedia of Genes and Genomes (KEGG) within the “clusterProfiler” package in R [16]. $P < 0.05$ was considered to indicate enrichment.

Stemness score

The “stemness” gene set was downloaded from the Molecular Signatures database (<https://www.gsea-msigdb.org/gsea/msigdb>) [17]. Gene set variation analysis was performed using the “GSVA” package in R in order to estimate variation in stemness across different cell types in an unsupervised manner [18].

Pseudotime analysis

Monocle 3 was used to simulate an evolutionary trajectory through pseudotime [15]. The “importCDS” function in Monocle was used to convert the original count in the Seurat object into the “CellDataSet” data set, and the “differentialGeneTest” function was used to identify

genes that may help identify genes whose expression changes across pseudotime ($q_{\text{val}} < 0.01$). The “dimension reduction” function was used for clustering, while the “orderCells” function was used to infer the trajectory based on default parameters. Gene expression was mapped using the “plot_genes_pseudotime” function.

Cell-cell crosstalk between cell clusters

The iTALK package in R [19] was used to investigate cell-cell crosstalk between cell clusters. Briefly, the top 50% of highly expressed genes in each cell cluster were matched to the 2,648 non-redundant ligand-receptor pairs included in the iTALK package. These pairs fall into four categories, based on whether the ligand serves as a checkpoint protein, cytokine, growth factor, or “other” protein. The top 20 ligand-receptor pairs for each type were visualized as a ligand-receptor interaction network.

Gene regulatory network and regulons

We used a modified version of the “Single-Cell Regulatory Network Inference” (SCENIC) approach [20, 21] to construct a gene regulatory network from the single-cell RNA sequencing data [22]. First, co-expression modules of transcription factors (TFs) and their potential target genes were identified. Second, the most likely target genes were identified based on enrichment of the appropriate binding motifs in the TFs. The resulting regulons of TFs with their most likely target genes were assigned a “regulon activity score” (RAS) in each single cell, based on the area under the receiver operating characteristic curve.

The bioinformatical analysis on the bulk data level

The microarray data of UC patients and controls have been downloaded from the Gene Expression Omnibus (GEO) database (accession number: GSE38713, the platform: GPL570) [23]. The bulk data from intestinal mucosa of 13 healthy controls and 30 UC patients. The differentially expressed genes were identified using the Linear Models for Microarray data (limma) package [24] in R software. $P < 0.05$ was considered to indicate a statistically significant difference.

Molecular docking

Molecular docking studies of different cell types via surface receptors and ligands were performed using Hex8.0.0.0 software [25] and protein crystal structures available in the Protein Database (<https://www.rcsb.org/pages/contactus>) [26]. Binding energy < 0 was taken to indicate possible binding. Potential complexes were visualized with Pymol software [27].

RESULTS

Total cellular landscape in UC

The sampling, sequencing and analysis workflow was shown in Figure 1A. Through single-cell RNA sequencing of 68 colonoscopy specimens from 18 patients with UC and 12 healthy individuals, 366,650 high-quality cells were obtained. These cells were divided into 51 clusters based on the UMAP method. And we found that the distribution and number of cells of different subtypes was of difference (Figure 1B). The violin pictures of healthy individuals-specific marker genes for each cell type further supported these cell types (Figure 1C). In addition, the expression of marker genes common to UC patients and healthy controls was different in each cell type (Figure 1D). Furthermore, we identified marker genes specific to UC patients whose expression differed in UC patients and healthy controls (Figure 1E and Supplementary Table 1).

Immune cell landscape in UC

UC impairs the integrity of the intestinal mucosa, which can compromise host immune tolerance toward intestinal microbes. Therefore we examined the landscape of immune cells in UC. Analysis of the DEGs in 51 types of cells (Figure 2A) showed functional enrichment in pathways involving immunity, apoptosis and inflammation, including pathways mediated by NF- κ B, IL-17, PPAR, ErbB, and T cell receptors (Figure 2B). We also found that immune cells may communicate with each other via binding between surface receptors and their cognate ligands (Figure 2C). In particular, iTALK predicted that macrophages may communicate with Best4⁺ enterocytes, enterocytes and immature enterocytes (Supplementary Table 2). The interactions among the function pathways and genes in enterocytes of the above three subtypes were identified (Supplementary Tables 4–6). Interestingly, we found that some receptor or ligand genes (ITGB1, CD44, VCAN, CD4, ITGB2, AXL, CANX and PLAUR) were significantly highly expressed in UC patients compared with healthy controls based on the bulk data (Supplementary Table 3).

Single-cell atlas of ADMSCs

High-quality transcriptome data were obtained from 24,358 single ADMSCs (Figure 3A). UMAP dimensionality reduction showed that the cells were divided into four clusters (Figure 3B). The stemness score of 4 clusters was calculated, the Cluster 3 showed the highest stemness score, while clusters 1 and 2 showed the lowest (Figure 3C). Pseudo-time analysis suggested that ADMSCs in clusters 0, 1 and 2 differentiated from the cells in clusters 3 (Figure 3D).

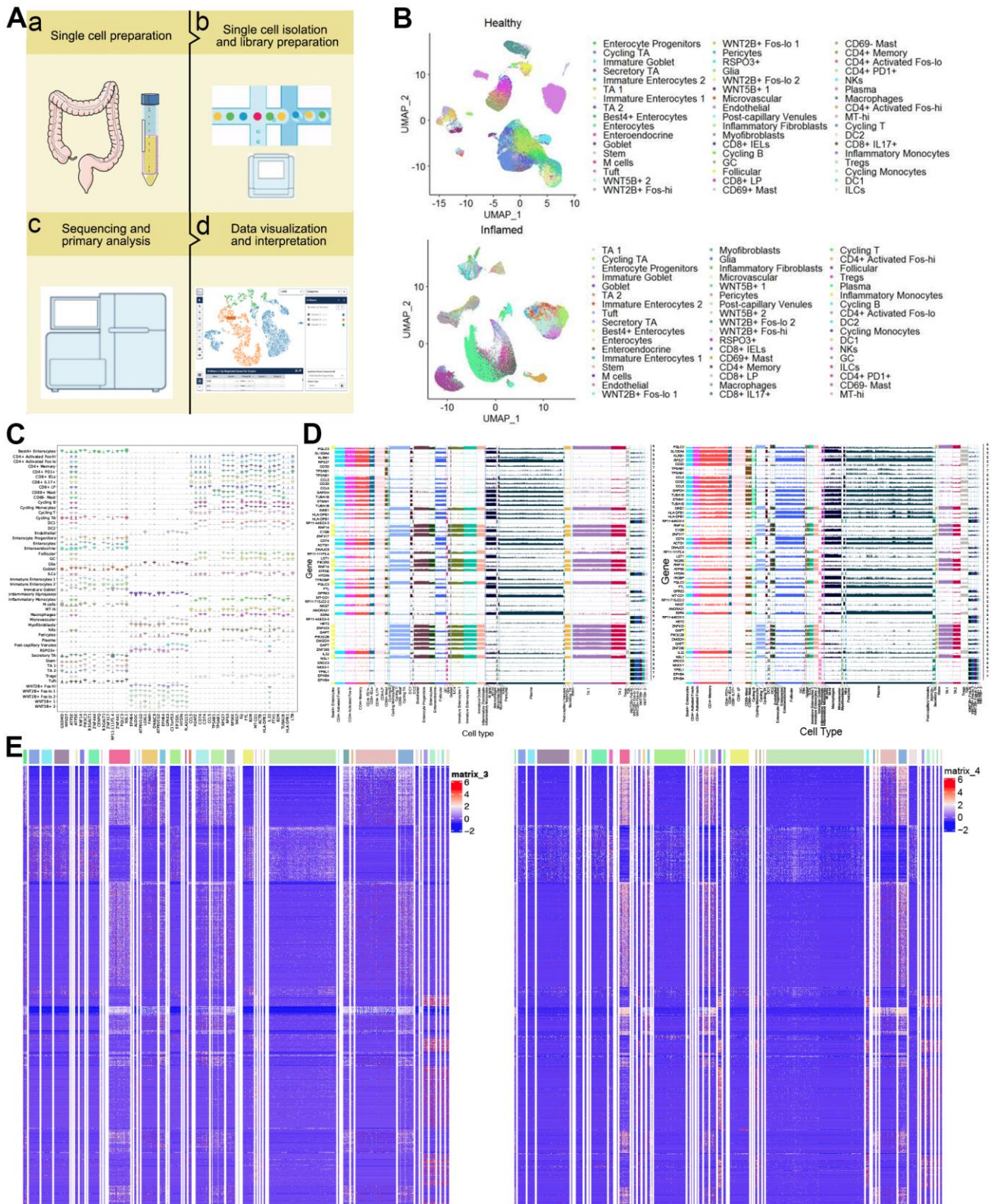


Figure 1. Single-cell transcriptomic profiles from colon biopsies from UC patients and healthy individuals. (A) Study design. **(B)** 2d visualization of 51 clusters of cells in healthy controls (up) and UC patients (down) on the UMAP plot. **(C)** Violin plots of specific marker genes in all types in healthy individuals. **(D)** Ridge plot. Expression of marker genes common to healthy individuals (left) and UC patients (right). **(E)** The heat map showing expression of UC-specific marker genes in healthy individuals (left) and UC patients (right). UMAP: uniform manifold approximation and projection for dimension reduction. UC: ulcerative colitis.

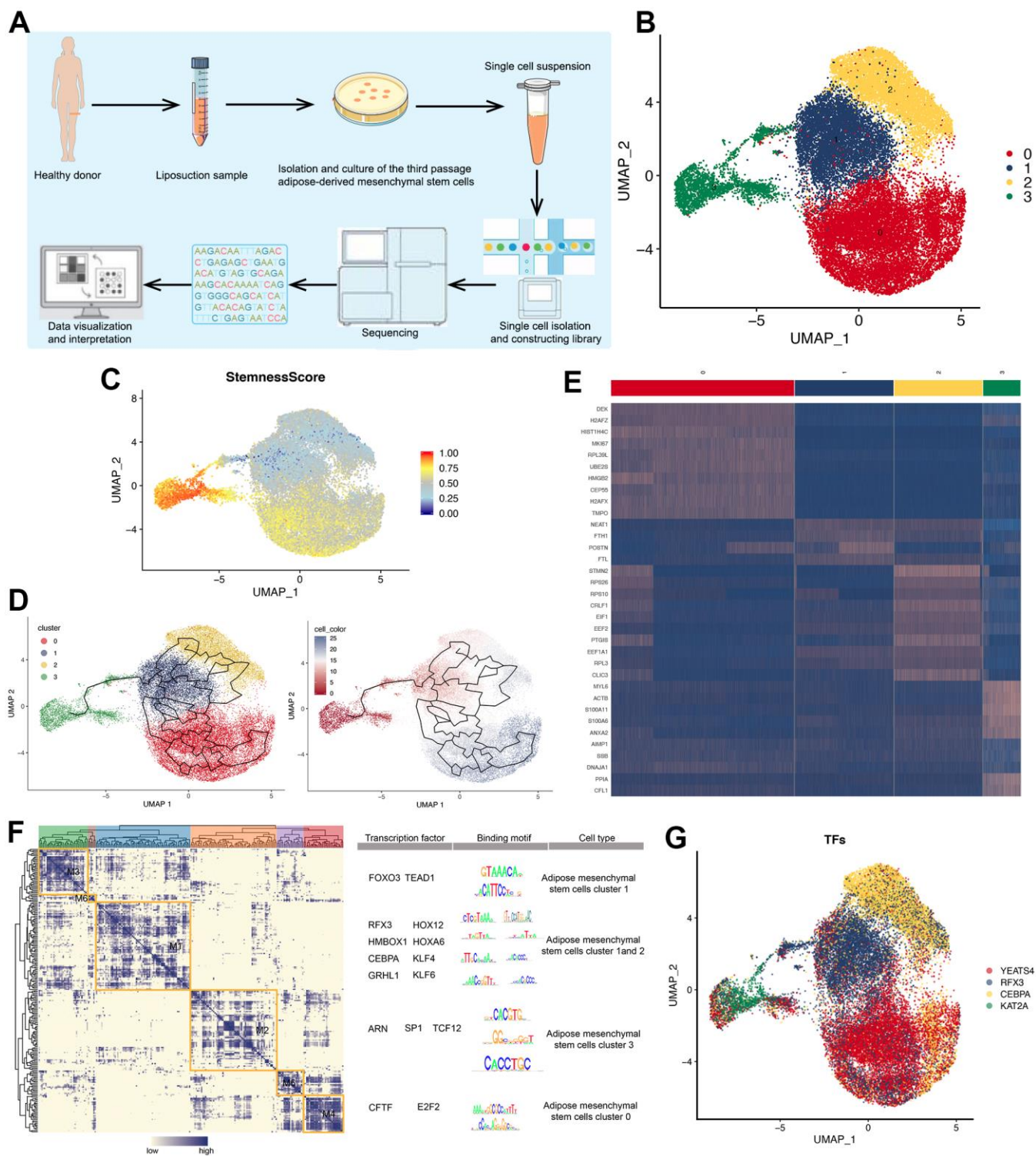


Figure 3. Single-cell atlas of ADMSCs. (A) Flow chart of sampling, sequencing and analysis of ADMSCs in this study. (B) 2D visualization of four clusters of 24,258 ADMSCs on the UMAP plot. (C) 2D visualization of stemness score of four cluster of ADMSCs on the UMAP plot. (D) Pseudotime developmental trajectory of ADMSCs shown in the UMAP plot. (E) Heat map, showing the expression of specific marker genes in each cluster of ADMSCs. (F) Regulon modules identified based on the regulon CSI matrix. The right panel shows representative transcription factors, their binding motifs, and associated cell types. (G) UMAP plot, showing the expression of transcription factors in each ADMSC cluster. ADMSCs: adipose-derived mesenchymal stem cells. UMAP: uniform manifold approximation and projection for dimension reduction. CSI: connection specificity index.

which indicated nine potential ligand-receptor pairs (Figure 4D). Based on the findings in this study, we proposed a mechanism that ADMSCs may alleviate UC after enter into the human body through communicating with macrophages, thereby further communicating with enterocytes by ligand-receptor pairs (Figure 5).

DISCUSSION

In this bioinformatics study, we identified DEGs in different cell types of UC patients, which may participate in pathways involving immunity, apoptosis and inflammation. And we found that macrophages may communicate with enterocytes or ADMSCs. These

results may help guide future research into the onset, progression and treatment of UC.

Enrichment results of the DEGs identified in our study of UC showed that the signaling pathways were significantly with immunity, apoptosis and inflammation. In this study, MAPK, Ras and mTOR signaling pathway, as well as *E. coli*-related biological function were significantly enriched based on the DEGs in UC patients. MAPK cascade in turn participates in cell migration, differentiation and proliferation [28]. In addition, Ras proteins function as molecular switches in signaling pathways involved in cell differentiation, growth, migration, survival and proliferation [29].

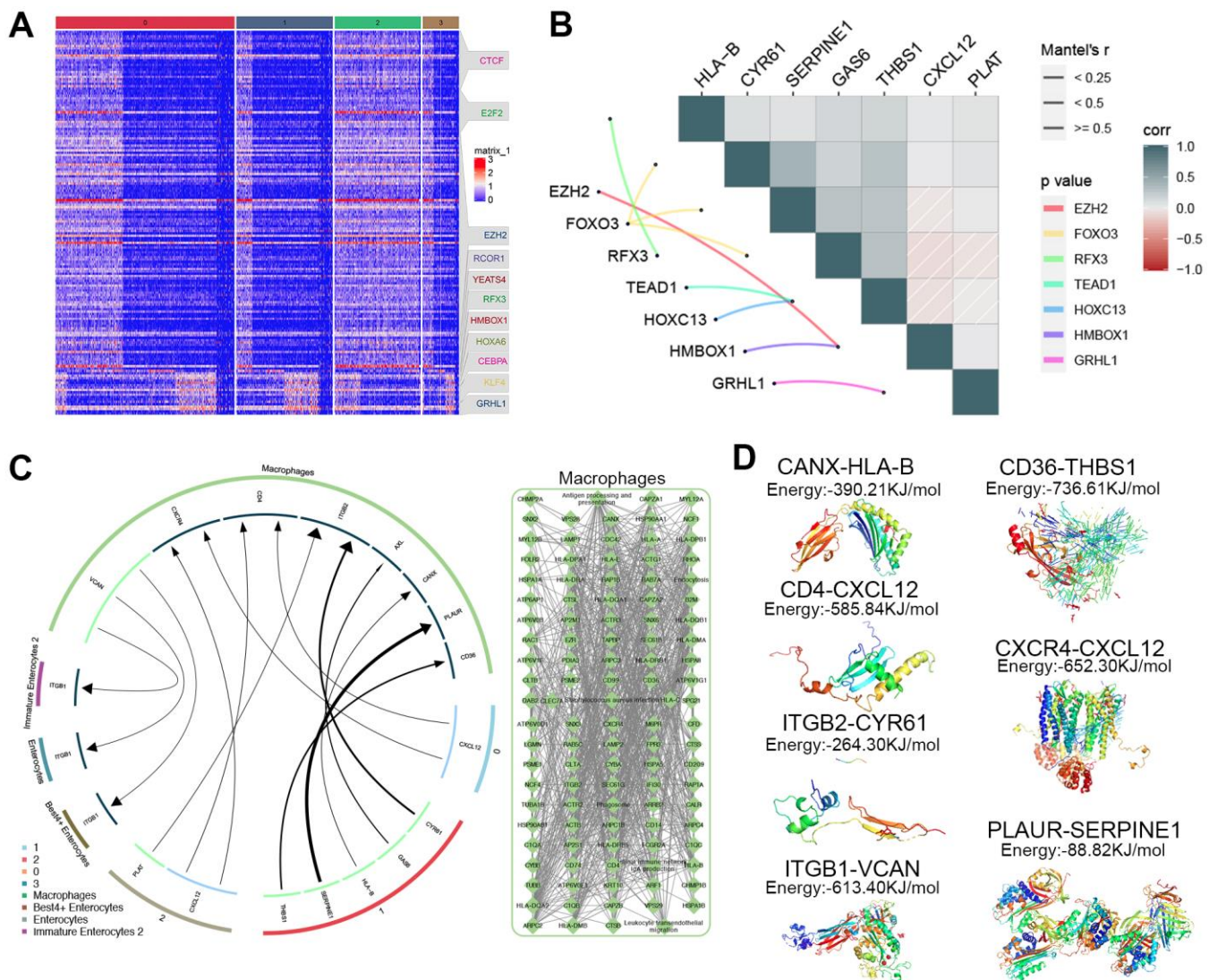


Figure 4. Exploration of how ADMSCs may alleviate UC. (A) Heat map, showing the expression of specific marker genes regulated by transcription factors in each ADMSCs cluster. (B) Correlation plot, showing relationships between transcription factors and ligands in ADMSCs. (C) Circos plot, showing relationships among macrophages, ADMSCs and three types of enterocytes. (D) Potential complexes between surface receptor and ligand obtained through molecular docking. ADMSCs: adipose-derived mesenchymal stem cells. UC:

apoptosis and autophagy [43, 44], while the TF TEAD1 may promote apoptosis and restrict proliferation [45]. The consistency between our bioinformatics analyses of ADMSCs and previous biological studies suggests the reliability of our approach.

There are some limitations in this study. On the other hand, the data in this study come from a relatively small sample and were analyzed using only bioinformatics techniques, but they provide a useful reference for experimental work to clarify the pathogenesis of UC and develop effective treatments. On the other hand, the expression of genes in UC patients and healthy individuals was preliminarily validated on the bulk data level, the findings in this study needs to be validated in more bulk data or the biological experiments.

AUTHOR CONTRIBUTIONS

The guarantor of integrity of the entire study: Yufeng Lv, Qiong Song and Shaowen Mo; study design: Yufeng Lv, Qiong Song and Shaowen Mo; data analysis: Chengyu Huang, Mengxin Wei, Yixuan Chen and Ting Li; manuscript preparation: Nan Zhang; manuscript editing: Nan Zhang; manuscript review: Nan Zhang.

CONFLICTS OF INTEREST

The authors declare that they have no conflicts of interest.

FUNDING

This research received no specific grant from any funding agency in the public, commercial, or not-for-profit sectors.

REFERENCES

1. Smillie CS, Biton M, Ordovas-Montanes J, Sullivan KM, Burgin G, Graham DB, Herbst RH, Rogel N, Slyper M, Waldman J, Sud M, Andrews E, Velonias G, et al. Intra- and Inter-cellular Rewiring of the Human Colon during Ulcerative Colitis. *Cell*. 2019; 178:714–30.e22. <https://doi.org/10.1016/j.cell.2019.06.029> PMID:31348891
2. Ordás I, Eckmann L, Talamini M, Baumgart DC, Sandborn WJ. Ulcerative colitis. *Lancet*. 2012; 380:1606–19. [https://doi.org/10.1016/S0140-6736\(12\)60150-0](https://doi.org/10.1016/S0140-6736(12)60150-0) PMID:22914296
3. Yang C, Merlin D. Nanoparticle-Mediated Drug Delivery Systems For The Treatment Of IBD: Current Perspectives. *Int J Nanomedicine*. 2019; 14:8875–89. <https://doi.org/10.2147/IJN.S210315> PMID:32009785

4. Burge K, Gunasekaran A, Eckert J, Chaaban H. Curcumin and Intestinal Inflammatory Diseases: Molecular Mechanisms of Protection. *Int J Mol Sci*. 2019; 20:1912. <https://doi.org/10.3390/ijms20081912> PMID:31003422
5. Salvo Romero E, Alonso Cotoner C, Pardo Camacho C, Casado Bedmar M, Vicario M. The intestinal barrier function and its involvement in digestive disease. *Rev Esp Enferm Dig*. 2015; 107:686–96. <https://doi.org/10.17235/reed.2015.3846/2015> PMID:26541659
6. Wang J, Zhang C, Guo C, Li X. Chitosan Ameliorates DSS-Induced Ulcerative Colitis Mice by Enhancing Intestinal Barrier Function and Improving Microflora. *Int J Mol Sci*. 2019; 20:5751. <https://doi.org/10.3390/ijms20225751> PMID:31731793
7. Groschwitz KR, Hogan SP. Intestinal barrier function: molecular regulation and disease pathogenesis. *J Allergy Clin Immunol*. 2009; 124:3–20. <https://doi.org/10.1016/j.jaci.2009.05.038> PMID:19560575
8. Ge J, Li YJ, Liu AQ, Huang WY, Yang F, Ma L, Zhai HH. [Changes of intestinal mucosal barrier in mice with chronic ulcerative colitis]. *Zhonghua Yi Xue Za Zhi*. 2018; 98:3950–3. <https://doi.org/10.3760/cma.j.issn.0376-2491.2018.48.009> PMID:30669801
9. Tatiya-Aphiradee N, Chatuphonprasert W, Jarukamjorn K. Immune response and inflammatory pathway of ulcerative colitis. *J Basic Clin Physiol Pharmacol*. 2018; 30:1–10. <https://doi.org/10.1515/jbcpp-2018-0036> PMID:30063466
10. Porter RJ, Kalla R, Ho GT. Ulcerative colitis: Recent advances in the understanding of disease pathogenesis. *F1000Res*. 2020; 9:F1000. <https://doi.org/10.12688/f1000research.20805.1> PMID:32399194
11. Gren ST, Grip O. Role of Monocytes and Intestinal Macrophages in Crohn's Disease and Ulcerative Colitis. *Inflamm Bowel Dis*. 2016; 22:1992–8. <https://doi.org/10.1097/MIB.0000000000000824> PMID:27243595
12. Zhao H, Shang Q, Pan Z, Bai Y, Li Z, Zhang H, Zhang Q, Guo C, Zhang L, Wang Q. Exosomes From Adipose-Derived Stem Cells Attenuate Adipose Inflammation and Obesity Through Polarizing M2 Macrophages and Beiging in White Adipose Tissue. *Diabetes*. 2018; 67:235–47. <https://doi.org/10.2337/db17-0356> PMID:29133512

13. Liu X, Xiang Q, Xu F, Huang J, Yu N, Zhang Q, Long X, Zhou Z. Single-cell RNA-seq of cultured human adipose-derived mesenchymal stem cells. *Sci Data*. 2019; 6:190031.
<https://doi.org/10.1038/sdata.2019.31>
PMID:[30806636](https://pubmed.ncbi.nlm.nih.gov/30806636/)
14. Cheng J, Zhang J, Wu Z, Sun X. Inferring microenvironmental regulation of gene expression from single-cell RNA sequencing data using scMLnet with an application to COVID-19. *Brief Bioinform*. 2021; 22:988–1005.
<https://doi.org/10.1093/bib/bbaa327>
PMID:[33341869](https://pubmed.ncbi.nlm.nih.gov/33341869/)
15. Liu Z, Sun Z, Liu H, Niu W, Wang X, Liang N, Wang X, Wang Y, Shi Y, Xu L, Shi W. Single-cell transcriptomic analysis of eutopic endometrium and ectopic lesions of adenomyosis. *Cell Biosci*. 2021; 11:51.
<https://doi.org/10.1186/s13578-021-00562-z>
PMID:[33685511](https://pubmed.ncbi.nlm.nih.gov/33685511/)
16. Yu G, Wang LG, Han Y, He QY. clusterProfiler: an R package for comparing biological themes among gene clusters. *OMICS*. 2012; 16:284–7.
<https://doi.org/10.1089/omi.2011.0118>
PMID:[22455463](https://pubmed.ncbi.nlm.nih.gov/22455463/)
17. Liberzon A, Subramanian A, Pinchback R, Thorvaldsdóttir H, Tamayo P, Mesirov JP. Molecular signatures database (MSigDB) 3.0. *Bioinformatics*. 2011; 27:1739–40.
<https://doi.org/10.1093/bioinformatics/btr260>
PMID:[21546393](https://pubmed.ncbi.nlm.nih.gov/21546393/)
18. Hänzelmann S, Castelo R, Guinney J. GSEA: gene set variation analysis for microarray and RNA-seq data. *BMC Bioinformatics*. 2013; 14:7.
<https://doi.org/10.1186/1471-2105-14-7>
PMID:[23323831](https://pubmed.ncbi.nlm.nih.gov/23323831/)
19. Sun T, Liu Z, Yang Q. The role of ubiquitination and deubiquitination in cancer metabolism. *Mol Cancer*. 2020; 19:146.
<https://doi.org/10.1186/s12943-020-01262-x>
PMID:[33004065](https://pubmed.ncbi.nlm.nih.gov/33004065/)
20. Aibar S, González-Blas CB, Moerman T, Huynh-Thu VA, Imrichova H, Hulselmans G, Rambow F, Marine JC, Geurts P, Aerts J, van den Oord J, Atak ZK, Wouters J, Aerts S. SCENIC: single-cell regulatory network inference and clustering. *Nat Methods*. 2017; 14:1083–6.
<https://doi.org/10.1038/nmeth.4463> PMID:[28991892](https://pubmed.ncbi.nlm.nih.gov/28991892/)
21. Davie K, Janssens J, Koldere D, De Waegeneer M, Pech U, Kreft Ł, Aibar S, Makhzami S, Christiaens V, Bravo González-Blas C, Poovathingal S, Hulselmans G, Spanier KI, et al. A Single-Cell Transcriptome Atlas of the Aging *Drosophila* Brain. *Cell*. 2018; 174:982–98.e20.
<https://doi.org/10.1016/j.cell.2018.05.057>
PMID:[29909982](https://pubmed.ncbi.nlm.nih.gov/29909982/)
22. Han X, Wang R, Zhou Y, Fei L, Sun H, Lai S, Saadatpour A, Zhou Z, Chen H, Ye F, Huang D, Xu Y, Huang W, et al. Mapping the Mouse Cell Atlas by Microwell-Seq. *Cell*. 2018; 172:1091–107.e17.
<https://doi.org/10.1016/j.cell.2018.02.001>
PMID:[29474909](https://pubmed.ncbi.nlm.nih.gov/29474909/)
23. Planell N, Lozano JJ, Mora-Buch R, Masamunt MC, Jimeno M, Ordás I, Esteller M, Ricart E, Piqué JM, Panés J, Salas A. Transcriptional analysis of the intestinal mucosa of patients with ulcerative colitis in remission reveals lasting epithelial cell alterations. *Gut*. 2013; 62:967–76.
<https://doi.org/10.1136/gutjnl-2012-303333>
PMID:[23135761](https://pubmed.ncbi.nlm.nih.gov/23135761/)
24. Ritchie ME, Phipson B, Wu D, Hu Y, Law CW, Shi W, Smyth GK. limma powers differential expression analyses for RNA-sequencing and microarray studies. *Nucleic Acids Res*. 2015; 43:e47.
<https://doi.org/10.1093/nar/gkv007> PMID:[25605792](https://pubmed.ncbi.nlm.nih.gov/25605792/)
25. Macindoe G, Mavridis L, Venkatraman V, Devignes MD, Ritchie DW. HexServer: an FFT-based protein docking server powered by graphics processors. *Nucleic Acids Res*. 2010; 38:W445–9.
<https://doi.org/10.1093/nar/gkq311> PMID:[20444869](https://pubmed.ncbi.nlm.nih.gov/20444869/)
26. Burley SK, Berman HM, Kleywegt GJ, Markley JL, Nakamura H, Velankar S. Protein Data Bank (PDB): The Single Global Macromolecular Structure Archive. *Methods Mol Biol*. 2017; 1607:627–41.
https://doi.org/10.1007/978-1-4939-7000-1_26
PMID:[28573592](https://pubmed.ncbi.nlm.nih.gov/28573592/)
27. Mooers BH. Shortcuts for faster image creation in PyMOL. *Protein Sci*. 2020; 29:268–76.
<https://doi.org/10.1002/pro.3781> PMID:[31710740](https://pubmed.ncbi.nlm.nih.gov/31710740/)
28. Chen Z, Gibson TB, Robinson F, Silvestro L, Pearson G, Xu B, Wright A, Vanderbilt C, Cobb MH. MAP kinases. *Chem Rev*. 2001; 101:2449–76.
<https://doi.org/10.1021/cr000241p> PMID:[11749383](https://pubmed.ncbi.nlm.nih.gov/11749383/)
29. Karnoub AE, Weinberg RA. Ras oncogenes: split personalities. *Nat Rev Mol Cell Biol*. 2008; 9:517–31.
<https://doi.org/10.1038/nrm2438>
PMID:[18568040](https://pubmed.ncbi.nlm.nih.gov/18568040/)
30. Kennedy BK, Lamming DW. The Mechanistic Target of Rapamycin: The Grand Conductor of Metabolism and Aging. *Cell Metab*. 2016; 23:990–1003.
<https://doi.org/10.1016/j.cmet.2016.05.009>
PMID:[27304501](https://pubmed.ncbi.nlm.nih.gov/27304501/)
31. Pinaud L, Sansonetti PJ, Phalipon A. Host Cell Targeting by Enteropathogenic Bacteria T3SS Effectors. *Trends Microbiol*. 2018; 26:266–83.

- <https://doi.org/10.1016/j.tim.2018.01.010>
PMID:[29477730](https://pubmed.ncbi.nlm.nih.gov/29477730/)
32. Santos AS, Finlay BB. Bringing down the host: enteropathogenic and enterohaemorrhagic *Escherichia coli* effector-mediated subversion of host innate immune pathways. *Cell Microbiol.* 2015; 17:318–32.
<https://doi.org/10.1111/cmi.12412> PMID:[25588886](https://pubmed.ncbi.nlm.nih.gov/25588886/)
33. Liu H, Kai L, Du H, Wang X, Wang Y. LPS Inhibits Fatty Acid Absorption in Enterocytes through TNF- α Secreted by Macrophages. *Cells.* 2019; 8:1626.
<https://doi.org/10.3390/cells8121626> PMID:[31842409](https://pubmed.ncbi.nlm.nih.gov/31842409/)
34. Anand RJ, Dai S, Rippel C, Leaphart C, Qureshi F, Gribar SC, Kohler JW, Li J, Stolz DB, Sodhi C, Hackam DJ. Activated macrophages inhibit enterocyte gap junctions via the release of nitric oxide. *Am J Physiol Gastrointest Liver Physiol.* 2008; 294:G109–19.
<https://doi.org/10.1152/ajpgi.00331.2007>
PMID:[17975131](https://pubmed.ncbi.nlm.nih.gov/17975131/)
35. Fang B, Song Y, Liao L, Zhang Y, Zhao RC. Favorable response to human adipose tissue-derived mesenchymal stem cells in steroid-refractory acute graft-versus-host disease. *Transplant Proc.* 2007; 39:3358–62.
<https://doi.org/10.1016/j.transproceed.2007.08.103>
PMID:[18089385](https://pubmed.ncbi.nlm.nih.gov/18089385/)
36. Sun M, Sun L, Huang C, Chen BC, Zhou Z. Induction of Macrophage M2b/c Polarization by Adipose Tissue-Derived Mesenchymal Stem Cells. *J Immunol Res.* 2019; 2019:7059680.
<https://doi.org/10.1155/2019/7059680>
PMID:[31321244](https://pubmed.ncbi.nlm.nih.gov/31321244/)
37. Walters JR, Howard A, Rumble HE, Prathalingam SR, Shaw-Smith CJ, Legon S. Differences in expression of homeobox transcription factors in proximal and distal human small intestine. *Gastroenterology.* 1997; 113:472–7.
<https://doi.org/10.1053/gast.1997.v113.pm9247466>
PMID:[9247466](https://pubmed.ncbi.nlm.nih.gov/9247466/)
38. Wu F, Wu S, Tong H, He W, Gou X. HOXA6 inhibits cell proliferation and induces apoptosis by suppressing the PI3K/Akt signaling pathway in clear cell renal cell carcinoma. *Int J Oncol.* 2019; 54:2095–105.
<https://doi.org/10.3892/ijo.2019.4789> PMID:[31081053](https://pubmed.ncbi.nlm.nih.gov/31081053/)
39. Sousa L, Pankonien I, Simões FB, Chanson M, Amaral MD. Impact of KLF4 on Cell Proliferation and Epithelial Differentiation in the Context of Cystic Fibrosis. *Int J Mol Sci.* 2020; 21:6717.
<https://doi.org/10.3390/ijms21186717>
PMID:[32937756](https://pubmed.ncbi.nlm.nih.gov/32937756/)
40. Syafruddin SE, Rodrigues P, Vojtasova E, Patel SA, Zaini MN, Burge J, Warren AY, Stewart GD, Eisen T, Bihary D, Samarajiwa SA, Vanharanta S. A KLF6-driven transcriptional network links lipid homeostasis and tumour growth in renal carcinoma. *Nat Commun.* 2019; 10:1152.
<https://doi.org/10.1038/s41467-019-09116-x>
PMID:[30858363](https://pubmed.ncbi.nlm.nih.gov/30858363/)
41. Rowbotham K, Haugen J, Milavetz B. Differential SP1 interactions in SV40 chromatin from virions and minichromosomes. *Virology.* 2020; 548:124–31.
<https://doi.org/10.1016/j.virol.2020.06.012>
PMID:[32838933](https://pubmed.ncbi.nlm.nih.gov/32838933/)
42. Zhang R, Wang L, Pan JH, Han J. A critical role of E2F transcription factor 2 in proinflammatory cytokines-dependent proliferation and invasiveness of fibroblast-like synoviocytes in rheumatoid Arthritis. *Sci Rep.* 2018; 8:2623.
<https://doi.org/10.1038/s41598-018-20782-7>
PMID:[29422529](https://pubmed.ncbi.nlm.nih.gov/29422529/)
43. Brunet A, Bonni A, Zigmond MJ, Lin MZ, Juo P, Hu LS, Anderson MJ, Arden KC, Blenis J, Greenberg ME. Akt promotes cell survival by phosphorylating and inhibiting a Forkhead transcription factor. *Cell.* 1999; 96:857–68.
[https://doi.org/10.1016/s0092-8674\(00\)80595-4](https://doi.org/10.1016/s0092-8674(00)80595-4)
PMID:[10102273](https://pubmed.ncbi.nlm.nih.gov/10102273/)
44. Lehtinen MK, Yuan Z, Boag PR, Yang Y, Villén J, Becker EB, DiBacco S, de la Iglesia N, Gygi S, Blackwell TK, Bonni A. A conserved MST-FOXO signaling pathway mediates oxidative-stress responses and extends life span. *Cell.* 2006; 125:987–1001.
<https://doi.org/10.1016/j.cell.2006.03.046>
PMID:[16751106](https://pubmed.ncbi.nlm.nih.gov/16751106/)
45. Tome-Garcia J, Erfani P, Nudelman G, Tsankov AM, Katsyv I, Tejero R, Zhang B, Walsh M, Friedel RH, Zaslavsky E, Tsankova NM. Analysis of chromatin accessibility uncovers TEAD1 as a regulator of migration in human glioblastoma. *Nat Commun.* 2018; 9:4020.
<https://doi.org/10.1038/s41467-018-06258-2>
PMID:[30275445](https://pubmed.ncbi.nlm.nih.gov/30275445/)

SUPPLEMENTARY MATERIALS

Supplementary Tables

Please browse Full Text version to see the data of Supplementary Tables 1, 4–6.

Supplementary Table 1. The differentially expressed genes in UC patients and controls.

Supplementary Table 2. The receptor and ligand pairs of macrophages and enterocytes of different subtypes.

Ligand	Receptor	Cell_from_mean_exprs	Cell_from	Cell_to_mean_exprs	Cell_to
VIM	CD44	392.9345568	1	0.639843532	Macrophages
COL1A1	CD44	214.0378432	1	0.639843532	Macrophages
COL1A2	CD44	117.4523317	2	0.639843532	Macrophages
FN1	CD44	76.85261818	2	0.639843532	Macrophages
COL1A1	CD36	135.694858	0	0.340597932	Macrophages
APP	CD74	1.95886416	0	17.00223526	Macrophages
COL1A1	CD44	31.21820918	3	0.639843532	Macrophages
FN1	PLAUR	26.22723853	3	0.566359318	Macrophages
PKM	CD44	23.19493477	0	0.639843532	Macrophages
VCAN	CD44	7.218096458	1	0.639843532	Macrophages
FGF2	CD44	4.701765157	0	0.639843532	Macrophages
THBS1	CD36	6.203453569	0	0.340597932	Macrophages
CTGF	ITGB2	2.679834462	3	0.664291702	Macrophages
SPON2	ITGB2	2.673404425	2	0.664291702	Macrophages
ANXA1	FPR3	6.580932675	2	0.250209556	Macrophages
TGFB1	CXCR4	4.411153791	1	0.293657446	Macrophages
THBS1	CD36	3.579759217	3	0.340597932	Macrophages
GAS6	AXL	7.75743349	1	0.134534786	Macrophages
GAS6	AXL	4.842440522	0	0.134534786	Macrophages
HLA-B	CANX	1.37237145	0	0.35582565	Macrophages
CXCL12	CXCR4	1.493169609	0	0.293657446	Macrophages
CSF1	CSF1R	0.836543053	2	0.289466331	Macrophages
CSF1	CSF1R	0.587797391	0	0.289466331	Macrophages
PROS1	AXL	0.358109184	2	0.134534786	Macrophages
ICAM3	ITGB2	0.062829195	3	0.664291702	Macrophages
VCAN	ITGB1	0.654512434	Macrophages	0.462867012	Best4+ Enterocytes
VCAN	ITGB1	0.654512434	Macrophages	0.4375	Enterocytes
VCAN	ITGB1	0.654512434	Macrophages	0.498440424	Immature Enterocytes 2

Supplementary Table 3. The expression levels of the differentially expressed receptor or ligand genes obtained in bulk data through single cell analysis.

Symbol	LogFC	AveExpr	t	P.Value	adj.P.Val	B
ITGB1	0.014940634	3.782862	2.2946137	0.026785722	0.146494886	-4.382364
CD44	0.1351186	3.507543	5.180855	5.81345E-06	0.000540562	3.604434
VCAN	0.2244977	2.672022	3.40536	0.001458855	0.01869735	-1.709587
CD4	0.08734719	2.941532	2.664814	1.09E-02	0.077302676	-3.5718828
ITGB2	0.22633679	3.022593	3.041501	0.004032696	0.03837442	-2.66088
AXL	0.150793	2.925003	2.495249	0.01657418	0.1042333	-3.954259
CANX	0.04339978	3.655007	5.314411	3.75E-06	0.000410103	4.031727
PLAUR	0.1633127	2.991897	3.309774	0.001915449	0.02262415	-1.96566
CD36	-0.1378495	2.660956	-2.070367	0.04456048	0.2074994	-4.827498
HLA-A	-0.003592468	3.834781	-0.467279	0.6426995	0.9354278	-6.784791
HLA-B	-0.01278865	3.844941	-0.8690066	0.3897497	0.7887466	-6.515917
HLA-C	-0.01500723	3.70149	-0.9425641	0.3512585	0.7486185	-6.449699
CXCR4	0.1313991	3.17712	1.456362	0.1526787	0.4684196	-5.846819

Supplementary Table 4. The interactions among the enriched pathways and the differentially expressed genes in Best4+ enterocytes.

Supplementary Table 5. The interactions among the enriched pathways and the differentially expressed genes in enterocytes.

Supplementary Table 6. The interactions among the enriched pathways and the differentially expressed genes in immature enterocytes 2.